

5-1-2018

Mice harbouring an oculodentodigital dysplasia-linked Cx43 G60S mutation have severe hearing loss

Julia M. Abitbol

University of Western Ontario, Department of Anatomy and Cell Biology

John J. Kelly

University of Western Ontario, Department of Anatomy and Cell Biology

Kevin J. Barr

University of Western Ontario, Department of Anatomy and Cell Biology

Brian L. Allman

University of Western Ontario, Department of Anatomy and Cell Biology

Dale W. Laird

University of Western Ontario, Department of Anatomy and Cell Biology, dale.laird@schulich.uwo.ca

Follow this and additional works at: <https://ir.lib.uwo.ca/anatomypub>



Part of the [Anatomy Commons](#), and the [Cell and Developmental Biology Commons](#)

Citation of this paper:

Abitbol, Julia M.; Kelly, John J.; Barr, Kevin J.; Allman, Brian L.; and Laird, Dale W., "Mice harbouring an oculodentodigital dysplasia-linked Cx43 G60S mutation have severe hearing loss" (2018). *Anatomy and Cell Biology Publications*. 249.

<https://ir.lib.uwo.ca/anatomypub/249>

RESEARCH ARTICLE

Mice harbouring an oculodentodigital dysplasia-linked Cx43 G60S mutation have severe hearing loss

Julia M. Abitbol, John J. Kelly, Kevin J. Barr, Brian L. Allman* and Dale W. Laird*[‡]

ABSTRACT

Given the importance of connexin43 (Cx43, encoded by *GJA1*) function in the central nervous system and sensory organ processing, we proposed that it would also be crucial in auditory function. To that end, hearing was examined in two mouse models of oculodentodigital dysplasia that globally express *GJA1* mutations resulting in mild or severe loss of Cx43 function. Although Cx43^{I130T/+} mutant mice, with ~50% Cx43 channel function, did not have any hearing loss, Cx43^{G60S/+} mutant mice, with ~20% Cx43 channel function, had severe hearing loss. There was no evidence of inner ear sensory hair cell loss, suggesting that the mechanism for Cx43-linked hearing loss lies downstream in the auditory pathway. Since evidence suggests that Cx26 function is essential for hearing and may be protective against noise-induced hearing loss, we challenged Cx43^{I130T/+} mice with a loud noise and found that they had a similar susceptibility to noise-induced hearing loss to that found in controls, suggesting that decreased Cx43 function does not sensitize the mice for environmentally induced hearing loss. Taken together, this study suggests that Cx43 plays an important role in baseline hearing and is essential for auditory processing.

This article has an associated First Person interview with the first author of the paper.

KEY WORDS: Cx43, Connexin, Gap junction, Hearing loss, Noise exposure

INTRODUCTION

Connexin (Cx) gap junction proteins form channels that allow for direct intercellular communication via the passage of small molecules and ions between contacting cells (Bruzzone et al., 1996; Laird, 1996, 2006). Although less understood *in vivo*, connexins may occasionally act as hemichannels at the cell surface to allow for transient exchange of small molecules between the cell cytosol and the extracellular environment (Goodenough et al., 1996). Gap junctional intercellular communication (GJIC) is essential for the maintenance of key cellular processes such as apoptosis, proliferation and differentiation in many tissues in the body, including the inner ear (Kikuchi et al., 1994, 1995). Gap junctions are critical in hearing as they form two specific networks in the cochlea; the epithelial and connective tissue gap junction networks (Forge et al., 1999; Kikuchi et al., 2000b).

These networks allow passage of small molecules and ions throughout the syncytium, and are thought to play roles in K⁺ buffering and metabolite transport (Chang et al., 2008; Kikuchi et al., 2000a). Gap junction channels are also thought to maintain ionic homeostasis through recycling of small molecules and secondary messengers within the cochlear duct (Jagger and Forge, 2006, 2015; Nickel and Forge, 2008). In addition, connexin hemichannels may play a role in hair cell maturation and development, through release of Ca²⁺ and ATP which are both required in early stages of hair cell development (Anselmi et al., 2008; Johnson et al., 2017; Piazza et al., 2007; Verselis, 2017).

The auditory system is broadly divided into two subcategories; the peripheral auditory system, which is made up of the outer (ear canal and eardrum), middle (middle ear bones) and inner (cochlea) ear, and the central auditory system, which consists of the neurons that ultimately connect the mechanosensory hair cells in the cochlea to the brain. The auditory system is known to express multiple connexin family members including Cx26, Cx30, Cx31, Cx29 (the equivalent of Cx30.2 in human), Cx32 and Cx43 (encoded in humans by *GJB2*, *GJB6*, *GJB3*, *GJC3*, *GJB1* and *GJA1*, respectively), which are all expressed in various locations along the auditory tract (Forge et al., 1999; Kikuchi et al., 2000b). Importantly, the two types of mechanosensory hair cells, which either amplify sound coming into the cochlea ('outer' hair cells) or transform sound waves into electrical signals ('inner' hair cells) within an area of the cochlea called the organ of Corti, are devoid of any known connexins (Kikuchi et al., 1995; Zhao and Santos-Sacchi, 1999). Cx26 and Cx30, which are the most abundant connexins in the inner ear, form the two gap junction networks in the cochlea, and have therefore been the most-studied connexins within the auditory system. Mutations in the genes encoding Cx26 are prevalent in patients with inherited hearing loss. Over 100 different gain or loss-of-function *GJB2* (Cx26) gene mutations have been identified. In addition, mice harbouring both ablations and/or mutations in *Gjb2* and *Gjb6* (Cx30) have hearing deficits as well as, in some cases, altered cochlear morphology (Cohen-Salmon et al., 2002; Crispino et al., 2011; Kudo et al., 2003; Sun et al., 2009; Teubner et al., 2003; Wang et al., 2009). Thus, due to the prevalence of *GJB2* and *GJB6* mutations in hearing loss, there is a strong need to identify molecules that can regulate connexin expression or function as a possible means to compensate for genetic deficiencies caused by connexin gene mutations.

Cx43 is the most ubiquitously expressed connexin family member in the body and has been documented in various regions of the auditory tract including the stria vascularis, supporting cells (Lautermann et al., 1998), spiral ligament (Locher et al., 2015), and Schwann and satellite cells of the spiral ganglion neurons (Liu et al., 2009, 2014; Liu and Yang, 2015), all of which reside within the inner ear. In addition, Cx43 has been found in the cochlear bone that encapsulates the cochlea (Cohen-Salmon et al., 2004) as well as in cells that reside in the auditory brainstem and midbrain relays (eighth cranial nerve, cochlear nucleus, olivary complex, lateral

University of Western Ontario, Department of Anatomy and Cell Biology, London, Ontario, Canada, N6A 5C1.

*These authors contributed equally to this work

[‡]Author for correspondence (dale.laird@schulich.uwo.ca)

 D.W.L., 0000-0002-4568-3285

Received 20 December 2017; Accepted 27 March 2018

lemniscus and the inferior colliculus) that are responsible for propagation of electrical signals throughout the brain (Ball et al., 2007; Kim et al., 2013). Although studies have identified Cx43 in these different regions along the auditory tract, its functional role and link to hearing remains unclear. A few studies have examined the prevalence of Cx43 mutations in patients harbouring hearing loss, with variable findings. In a group of Taiwanese patients with hearing loss, *GJAI* (Cx43) gene mutations were found to be the second most common after *GJB2* (Cx26) mutations (Yang et al., 2007). However, other studies have found no evidence of Cx43 mutations in Turkish and African patients with hearing loss (Bosch et al., 2014; Uyguner et al., 2003; Wonkam et al., 2015). Interestingly, two recessive gene mutations in *GJAI* leading to L11F and V24A amino acid substitutions in the cytoplasmically exposed N-terminal domain and the first transmembrane domain of Cx43, respectively, have been discovered in human patients and linked to non-syndromic hearing loss (Liu et al., 2001).

In addition to genetic forms of hearing loss, environmental factors such as exposure to loud sound can lead to hearing impairments. Both Cx26 and Cx30, connexin family members that are critical for hearing, are thought to play a role in the active transport of Na⁺ and K⁺ within the cochlea to maintain its proper function and homeostasis (Kikuchi et al., 2000a). Recently, a study found that both Cx26 and Cx30 protein levels were significantly decreased after noise exposure (Yamaguchi et al., 2014). Since then, another study has shown that when Cx26 is conditionally knocked down at postnatal day 18, mice exhibit more pronounced noise-induced hearing loss than their wild-type (WT) counterparts (Zhou et al., 2016). At present, it is unknown whether patients harbouring *GJAI* mutations are more susceptible to auditory damage after a loud noise exposure.

Examining the functional roles of Cx43 in the auditory system has been hindered by the fact that global Cx43 knock-out mice are lethal at birth (Reaume et al., 1995). To overcome this limitation, it is now possible to use genetically modified mice to model human-linked Cx43 diseases, which typically manifest as the developmental abnormality known as oculodentodigital dysplasia (ODDD) (Paznekas et al., 2003, 2009; Shibayama et al., 2005). ODDD is a human-linked disease that is mostly inherited in an autosomal-dominant manner, where patients typically exhibit craniofacial abnormalities, fusion of soft tissue digits, small eyes, enamel defects and, in some rare cases, neurological defects and/or hearing loss (Paznekas et al., 2003). Previously, to assess the role of Cx43 in a wide variety of tissues and organs such as the skin, heart, mammary glands, bone and brain, Cx43^{I130T/+} and Cx43^{G60S/+} mice have been used, which reduce Cx43 function to ~50% and ~20% of controls, respectively (Flenniken et al., 2005; Kalcheva et al., 2007; Manias et al., 2008; Plante and Laird, 2008; Stewart et al., 2013). Given the different levels of Cx43 function in these mutant mice, they become excellent surrogates to assess the role of Cx43 in hearing as we postulate that hearing loss might be found in both mutant mice or only mice that have little remaining Cx43 function (i.e. the Cx43^{G60S/+} mice).

The aim of this study was to use mouse models of ODDD to investigate the impact of Cx43 in auditory function through various physiological assessments. First, we wanted to determine whether fully functional Cx43 is crucial for proper development of the auditory tract; second, we wanted to examine whether the level of functional Cx43-based GJIC impacts auditory function; and, finally, we wanted to determine whether the auditory system of Cx43 mutant mice is more susceptible to insult upon exposure to loud noise. We discovered that, although Cx43^{I130T/+} mutant mice had normal hearing that persisted in mature adult mice and after a

loud noise auditory insult, Cx43^{G60S/+} mutant mice had severe hearing loss, suggesting that hearing impairment is a result of severe loss of Cx43 function.

RESULTS

Cx43 mRNA transcript is expressed in the cochlea, and there is no evidence of compensation through increased transcription of Cx26 or Cx30 in Cx43 mutant mice

To confirm that Cx43 is expressed specifically in the cochlea, we used quantitative real-time RT-PCR (qRT-PCR) to determine the level of Cx43 in the cochlea of 2–3-month-old Cx43^{I130T/+}, Cx43^{G60S/+} mutant mice and their respective age- and sex-matched littermate controls. We found that Cx43 mRNA transcripts were similarly expressed in cochleae of Cx43^{I130T/+}, Cx43^{G60S/+} mutant mice and their WT littermate controls when normalized to 18S rRNA (Fig. S1A,B). Interestingly, both Cx26 and Cx30 mRNA transcripts were similarly expressed in cochleae of WT and Cx43 mutant mice with no evidence of compensation by Cx26 or Cx30 in Cx43^{I130T/+} or Cx43^{G60S/+} mutant mice at the mRNA level (Fig. S1C–F).

The total Cx43 protein level is lower in the cochleae of Cx43^{G60S/+} mutant mice

Total Cx43 protein levels were analysed in cochlear lysates obtained from dissected whole cochleae at various postnatal time points [postnatal day (P)4, P8, P14, and P30 and P60–P90]. Both strains of WT mice had a high abundance of total Cx43 protein expression at all developmental time points with both phosphorylated (P1/P2) and non-phosphorylated Cx43 species (NP) present (Fig. 1A,B). Cx43^{I130T/+} mutant mice appeared to have a lower level of Cx43 compared to their WT counterparts at all developmental time points; however, this difference was not significant when quantified for P60–P90 mice (Fig. 1A,C). Cx43^{G60S/+} mutant mice had an apparent reduction in Cx43 in the cochleae at every developmental time point and a significantly lower level of total Cx43 compared to WT littermates at the P60–P90 time point (Fig. 1B,D).

Cx43 is localized to cells of the cochlear nerve region

A clear understanding of the localization profile of Cx43 along the auditory tract remains controversial. In an attempt to resolve this issue, cochlear cross sections from WT and mutant mice were immunostained for Cx43. As might be expected, there was no detectable Cx43 (absence of red staining) in inner ear hair cells, which are demarcated by phalloidin staining of actin-rich stereocilia (green, Fig. 2A,B). Little Cx43 (denoted by red) was detected in the spiral ganglion neurons or in satellite cells surrounding the neurons, labelled by CNPase (green) (Fig. 2C). Further along the auditory pathway, Cx43 was highly expressed in the resident cells of the cochlear nerve region within the central modiolus, where all the spiral ganglion neurons are bundled together (Fig. 2D). Upon higher magnification imaging, Cx43 was found in distinct gap junction plaques in areas surrounding GFAP-positive cells, an astrocytic glial cell marker (green) (Fig. 2E,F, arrows). Cx43 gap junctions were also found between the cell processes, which formed a 'glial-like' syncytium in the cochlear nerve region (Fig. 2F). There was a noticeable reduction of Cx43 gap junctions in the cochlear nerve region of both mutant mice (Fig. 2E,F).

Cx43^{G60S/+} mutant mice have severe hearing loss and auditory brainstem deficits

To assess whether hearing in the mutant mice is directly influenced by the extent of Cx43 function, we utilized the auditory brainstem response (ABR) technique to measure hearing thresholds (i.e.

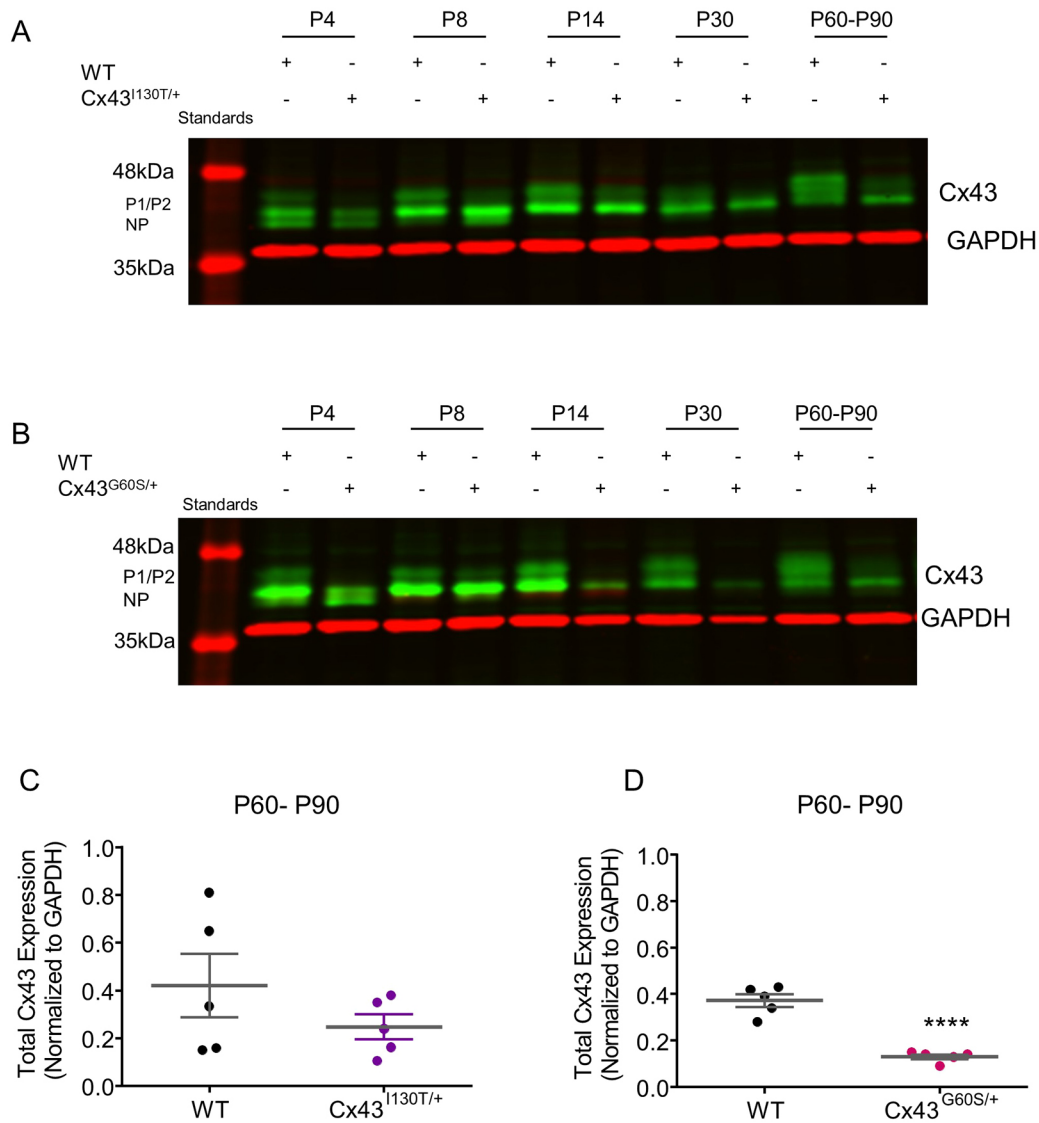


Fig. 1. Cx43 protein levels are reduced in Cx43^{G60S/+} mice. (A,B) Western blots revealed that Cx43 is prevalent in the cochlea of all mice, with mutant mice exhibiting variable amounts of the P1/P2 phosphorylated species. NP, not phosphorylated. (C,D) Total Cx43 levels (mean±s.e.m.) in the cochleae were quantified in mice at 2–3 months of age, and there were no differences in Cx43^{I130T/+} mice compared to controls (C), but there was a significant decrease in Cx43^{G60S/+} mutant mice compared to their WT littermates (D). $n=5$ pooled cochlear samples for each genotype. GAPDH was used as a loading control for western blots. **** $P<0.0001$ (independent Student's t -tests).

hearing sensitivity) in response to various acoustic stimuli. First, we administered a broad-band click stimulus to the animals, which activates several regions of the cochlear sensory epithelium and, thus, provides an overall measurement of hearing sensitivity. Second, we played specific tonal frequencies (4, 8, 16 and 24 kHz), that activate hair cells in specific regions of the cochlea, to give an indication of where along the sensory epithelium any dysfunction occurs. Representative examples of an ABR trace recording from WT and Cx43^{I130T/+} mutant mice showed similar waveform characteristics and thresholds in response to a click stimulus at decreasing sound intensity levels (90 to 30 dB sound pressure level, SPL; Fig. 3A). However, Cx43^{G60S/+} mutant mice had different waveform profiles, including decreased ABR amplitudes (indicating less synchronized neural firing in the auditory brainstem relays) and increased thresholds (i.e. worse hearing) compared to their WT littermate controls (Fig. 3B). Averaged ABR thresholds were similar for all stimuli tested in WT and Cx43^{I130T/+} mutant mice at

2–3 months of age (Fig. 3C). Normal hearing in Cx43^{I130T/+} mutant mice persisted in older mice at 6 months of age, albeit with an increase in ABR thresholds at higher frequencies, consistent with expected age-dependent high-frequency hearing loss due to their C57BL/6 background (Henry and Chole, 1980; Keithley et al., 2004; Mikaelian, 1979) (Fig. 3E). Although hearing remained intact in Cx43^{I130T/+} mutant mice, averaged ABR thresholds for all stimuli tested were significantly increased in Cx43^{G60S/+} mutant mice compared to their WT littermate controls at both 1 and 2–3 months of age (Fig. 3D,F) indicating that these mutant mice had severe hearing loss. ABR thresholds for Cx43^{G60S/+} mutant mice ranged from ~60–80 dB SPL compared to 20–40 dB SPL for WT littermate controls across all stimuli tested, showing a 40 dB elevation in hearing thresholds (i.e. worsened hearing) of Cx43^{G60S/+} mutant mice compared to their WT controls. Collectively, these data show that, although Cx43^{I130T/+} mutant mice have normal hearing, Cx43^{G60S/+} mutant mice have severe hearing loss.

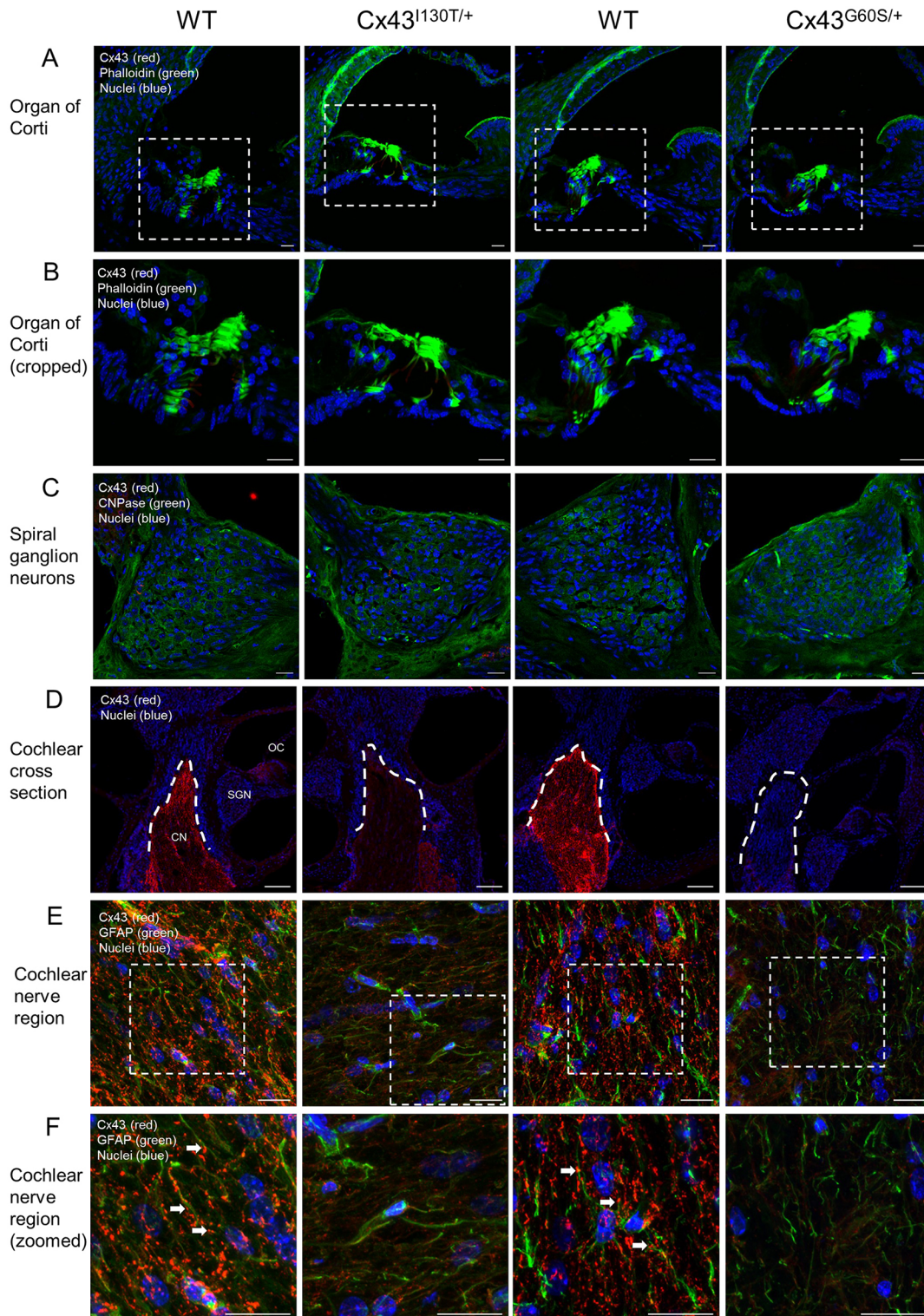


Fig. 2. Cx43 is highly expressed in a subset of cells within the cochlear nerve. (A,B) Immunofluorescence images revealed that Cx43 is not expressed in the cochlear duct region (red, Cx43; green, phalloidin staining of actin-rich stereocilia) (A) or in areas surrounding hair cells of the organ of Corti (B). (C) There was little to no detection of Cx43 in the spiral ganglion neurons (red, Cx43; green, Schwann cells). (D) Cx43 was found in the modiolus region of the cochlea (red, Cx43; blue, nuclei) and (E,F) was localized within GFAP-positive cells (green, GFAP; red, Cx43; blue, nuclei). OC, organ of Corti; SGN, spiral ganglion neurons; CN, cochlear nerve. The dashed line in D delineates the glial juncture of the cochlear nerve. The dashed box in E delineates the area shown in a magnified view in F. Arrows in F represent examples of Cx43 gap junction plaques in the cochlear nerve region. Scale bars: 20 μ m (A–C,E,F); 100 μ m (D).

In addition to measuring hearing sensitivity, ABR waveform morphologies provide an indication of the integrity of the ascending auditory pathway, where waves I–V correspond with the successive

relay centres (i.e. cochlear nerve, cochlear nucleus, superior olivary complex, lateral lemniscus and inferior colliculus, respectively). In order to examine whether Cx43 mutant mice had any defects in

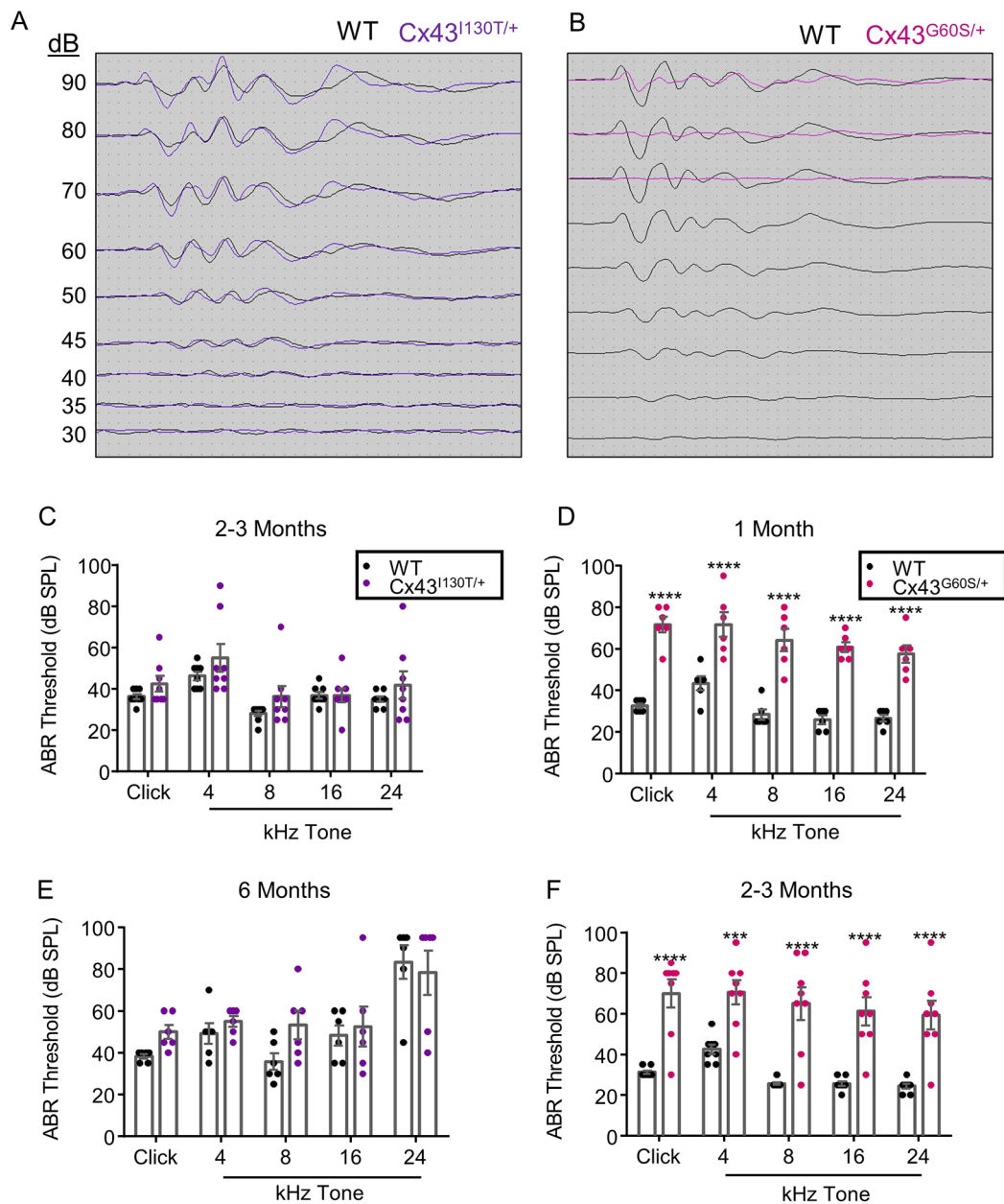


Fig. 3. Cx43^{G60S/+} mutant mice exhibit severe hearing loss. (A,B) Representative examples of a click stimulus recording for Cx43^{I130T/+}, Cx43^{G60S/+}, and their respective WT littermate controls overlaid together. (C–F) Mean \pm s.e.m. ABR thresholds for all stimuli in Cx43^{I130T/+} and Cx43^{G60S/+} mutant mice and their WT littermate controls. Cx43^{G60S/+} mutant mice had significantly elevated ABR thresholds (i.e. worse hearing) at both 1 and 2–3 months of age compared to their WT littermate controls (D,F). *** $P < 0.001$, **** $P < 0.0001$ (two-way repeated measures ANOVA). WT and Cx43^{I130T/+} mutant mice: $n = 8$ mice for 2–3 months and $n = 6$ mice for 6 months in each genotype. WT and Cx43^{G60S/+} mutant mice: $n = 6$ for 1 month and $n = 8$ for 2–3 months in each genotype.

specific auditory brainstem regions, we analysed the amplitudes and latencies of the loudest (90 dB SPL) click ABR waveforms to assess neural synchrony, where larger amplitude represents more synchronous neural firing, and latency represents the speed of neurons firing, respectively. Cx43^{I130T/+} mutant mice had similar ABR amplitudes and latencies to WT controls (Fig. 4A,C). Interestingly, Cx43^{G60S/+} mutant mice had significantly decreased ABR wave amplitudes but no difference in latencies, suggesting that Cx43-linked defects in neural synchrony and/or firing at those auditory brainstem regions but that it has no role in conduction speeds (Fig. 4B,D). Taken together, these results suggest that although Cx43^{I130T/+} mutant mice do not have auditory brainstem region deficits, Cx43^{G60S/+} mutant mice exhibit sensorineural hearing loss.

Hearing loss in Cx43^{G60S/+} mice is not due to reduced hair cell number or functional loss

Given that loss of hair cell number is a common cause of hearing impairment, we next assessed whether hearing loss in Cx43^{G60S/+} mice was due to inefficient development of the sensory epithelium. To this end, we cultured the organ of Corti from WT and Cx43 mutant pups (P0–P3) to visualize and count the number of hair cells. Representative images of organotypic cochlear cultures from WT and Cx43 mutant mice in each turn of the cochlea (apical, mid-apical, basal and mid-basal) showed that hair cells were intact in all mice, as visualized with the hair cell marker myosin VI (green), and the stereocilia marker phalloidin (red) (Fig. 5A). When the number of outer and inner hair cells were quantified from cochlear cultures,

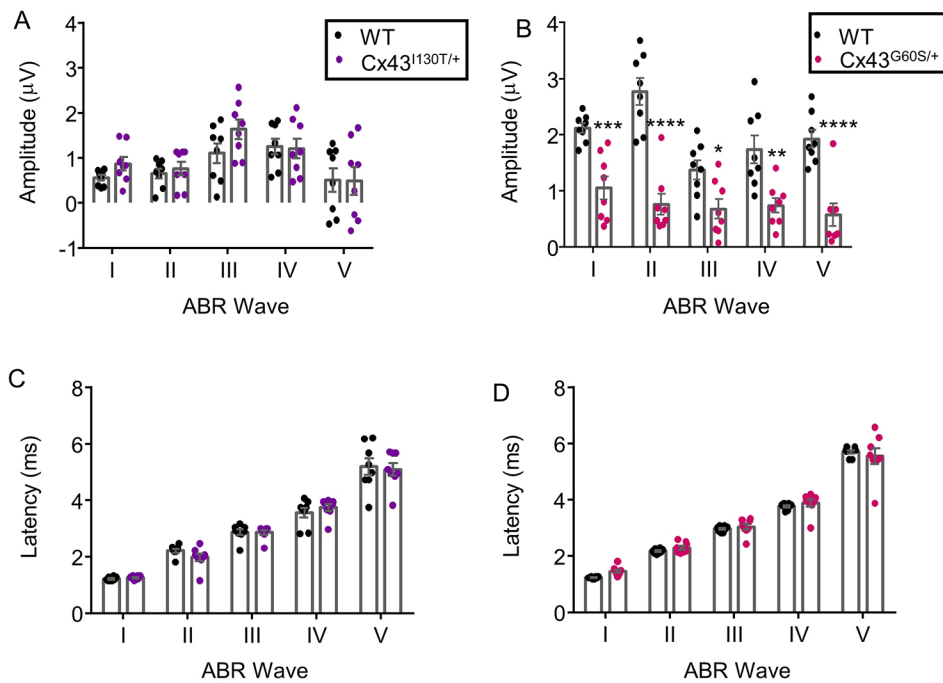


Fig. 4. Cx43^{G60S/+} mutant mice have decreased ABR waveform amplitudes. The amplitudes and latencies of all five ABR waveforms were analysed for a 90 dB SPL click stimulus. Cx43^{I130T/+} mutant mice had similar ABR wave amplitudes (neural firing/synchrony) and latencies (neural conduction speeds) for all five ABR waves compared to WT (A,C). However, Cx43^{G60S/+} mutant mice had significantly decreased ABR wave amplitudes compared to WT (B), although the ABR wave latencies remained the same (D). * $P < 0.05$, ** $P < 0.01$, *** $P < 0.001$, **** $P < 0.0001$ (two-way ANOVA); $n = 8$ mice per each cohort of each genotype. Bars represent mean \pm s.e.m.

there was no hair cell loss evident in Cx43^{I130T/+} or Cx43^{G60S/+} mutant mice in any of the cochlear regions (Fig. 5B).

Hair cell activation occurs via the deflection of hair-like stereocilia on the apical surface of hair cells in response to sound-induced vibration of the sensory epithelium (organ of Corti). The deflection causes the opening of mechanotransducer (MET) channels that allows the influx of cations, including K⁺, of which the concentration in endolymph is extremely high (150 mM). This leads to depolarization of hair cells and consequent Ca²⁺ uptake and neurotransmitter release. Taking advantage of this mechanism, we investigated whether hair cells in Cx43^{G60S/+} mice were functional by exposing cochlear cultures to the MET channel-permeable fluorescent FM1-43 dye. If MET channels are functional, the dye would enter hair cells and fluoresce green. Representative low (Fig. S2A) and high (Fig. 2SB) resolution images revealed that the rows of inner and outer hair cells of both Cx43 mutant and WT mice were able to take up the FM1-43 dye. Taken together, these organotypic cochlear culture results reveal that hearing loss in Cx43^{G60S/+} mutant mice is not due to hair cell damage in early postnatal development.

Although cochlear cultures from P0–P3 pups revealed that Cx43^{G60S/+} mutant mice did not have hair cell loss, hair cells at this stage are still immature and do not fully develop until \sim P14. Since Cx43^{G60S/+} mutant mice exhibited hearing loss at both 1 and 2–3 months of age, we assessed whether there was hair cell loss in adult (2–3 months old) mutant mice. Staining for hair cell markers, myosin VI and actin in whole-mount cochlear epithelium preparations of adult cochleae from the apical turns showed no evidence of hair cell loss, and the hair cells retained normal morphological appearances in Cx43^{G60S/+} mutant mice (Fig. 6A). Furthermore, to examine the structural integrity of the synaptic interface between the inner hair cells and the spiral ganglion neurons, we stained adult whole-mount sections with myosin VI to visualize hair cells, and CtBP2, a molecular marker expressed in ribbon synapses of hair cells that promotes rapid release of neurotransmitters to the spiral ganglion neurons. These dense ribbon synapses are essential for propagation of electrical signals to

the brainstem, and loss of such markers as CtBP2 can represent hearing loss. The inner hair cells of Cx43^{G60S/+} mutant mice appeared to have a similar number of CtBP2-positive synapses to controls suggesting no shortages in the innervation of inner hair cells (Fig. 6B).

Hearing loss in Cx43^{G60S/+} mice is not due to any evident spiral ganglion neuron degeneration or demyelination in the cochlear nerve region

Since there was no evidence of hair cell loss in the mutant mice, we next looked at spiral ganglion neuron morphology. There was no evidence of neuronal loss in Cx43^{G60S/+} mutant mice as evidenced by immunofluorescence labelling of β III tubulin, a neuronal marker, showing similar staining patterns in both WT and mutant mice (Fig. 7A). Furthermore, we examined whether Cx43^{G60S/+} mutant mice presented any evidence of differential expression of myelin in the modiolus region by using a marker for myelin, myelin basic protein. The cochlear nerve regions in both WT and Cx43^{G60S/+} mutant mice had abundant expression of myelin basic protein (Fig. 7B,C); however, whether there is more intricate disarrangement of myelin within the cochlear nerve region of Cx43^{G60S/+} mutant mice remains unknown.

WT and Cx43^{I130T/+} mutant mice have similar susceptibility to noise-induced hearing loss

To examine whether Cx43 plays a role in noise-induced hearing loss, we delivered a 12 kHz tonal stimulus at 115 dB SPL for 1 h to Cx43^{I130T/+} mutant mice and their WT littermate controls. Since reduced expression of Cx26, a known connexin family member that is required for hearing, has been shown to sensitize mice to noise-induced hearing loss, we postulated that mutant mice with reduced Cx43 function would be more susceptible to loud noise-induced hearing loss if Cx43 played a central role in this process. Hearing was measured by examining the ABRs at three separate time points: (1) baseline; (2) immediately after loud noise exposure; and (3) 1 week after noise exposure. While ABR thresholds remained similar for the low frequencies (Fig. 8A–C), as expected, thresholds were

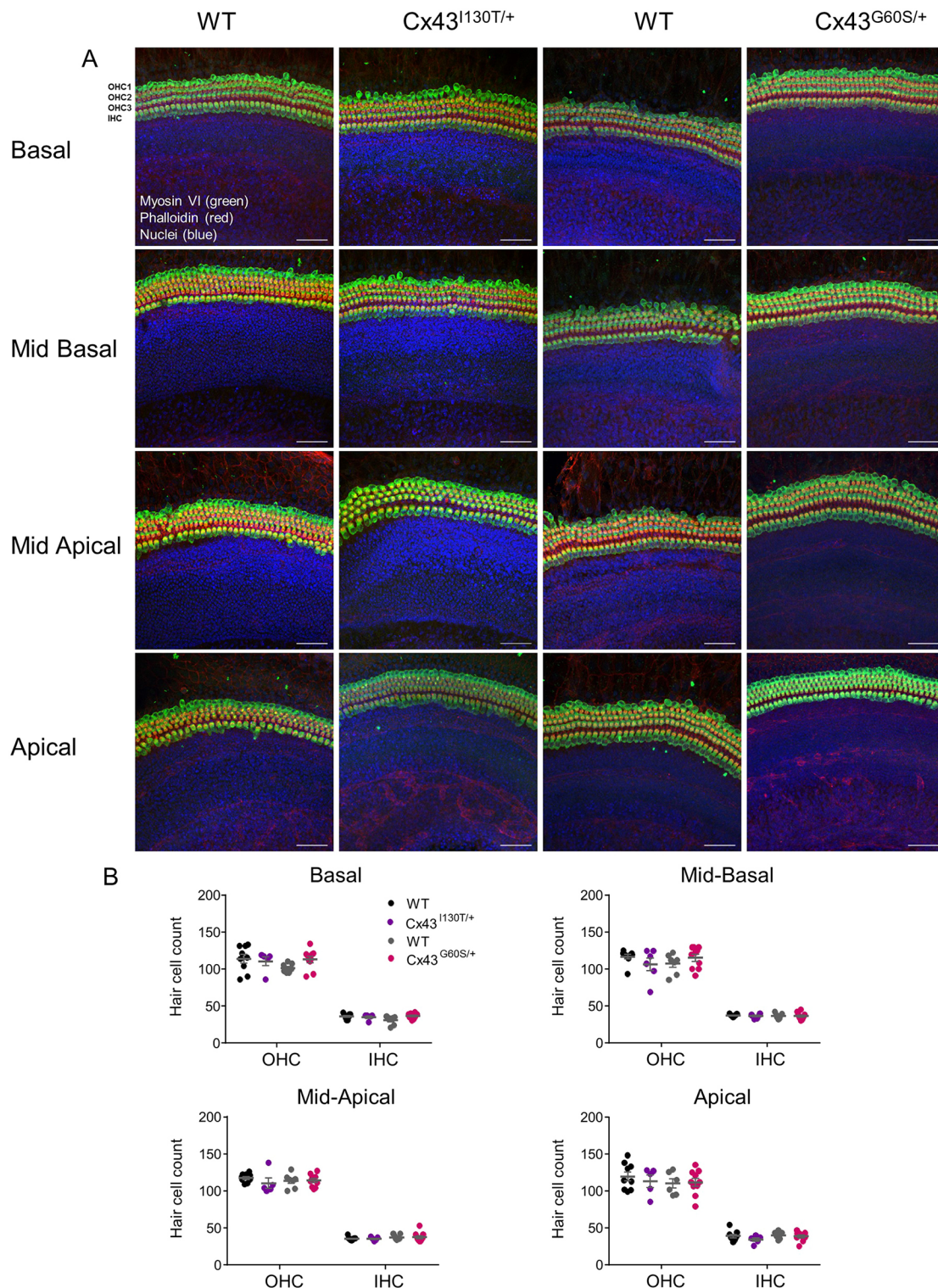


Fig. 5. Cx43^{G60S/+} mutant mice do not exhibit postnatal hair cell loss in cochlear cultures. (A) Representative confocal images of hair cell staining for each genotype of mice in four different regions of the cochlea, representing areas that respond to different frequency ranges. Basal, high frequency; Mid-Basal, mid-to-high frequencies; Mid-Apical, mid-to-low frequencies; Apical, low frequencies. Images were acquired on a 25 \times lens from 20 individual stacked slices (from the top to bottom span of the culture) and compiled to generate one merged image. Hair cell bodies were stained for myosin VI (green), and stereocilia of hair cells were stained with phalloidin (red). Blue, nuclei. (B) When the number of outer and inner hair cells were quantified for each cochlear region, there were no differences found in either Cx43 mutant mice compared to their WT littermate controls. OHC, outer hair cells; IHC, inner hair cells. Scale bars: 50 μ m.

elevated immediately after noise exposure in both WT and Cx43^{I130T/+} mice at the high (16 and 24 kHz) frequencies (Fig. 8D,E). With the exception of the broad-band click stimulus,

which only changed by \sim 10%, there were no differences in ABR thresholds between WT and Cx43^{I130T/+} mutant mice 1 week after noise exposure (Fig. 8A–E). Importantly, WT and Cx43^{I130T/+}

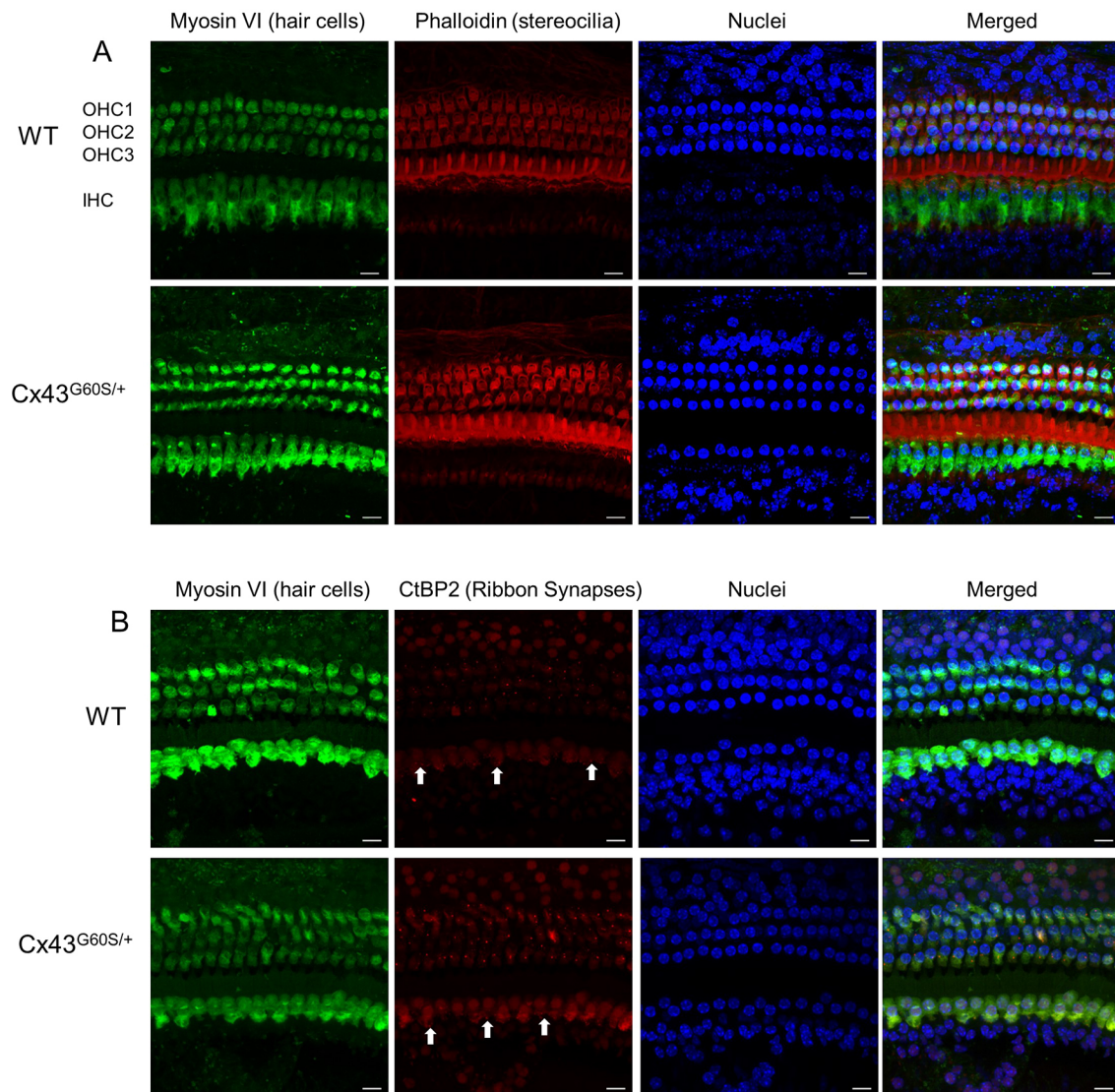


Fig. 6. Hair cells of $Cx43^{G60S/+}$ mutant mice remain intact in adult mice. (A) Hair cells dissected from the apical region of adult (2–3-month-old mice) cochleae labelled for myosin VI (green) and with phalloidin (red) revealed that hair cells were intact. Similarly, adult $Cx43^{G60S/+}$ mutant mice did not exhibit hair cell loss. (B) Adult whole mounts were also stained for hair cell-specific ribbon synapses using antibodies that target CtBP2 (red). Arrows indicate individual synapses that can be visualized. OHC, outer hair cells; IHC, inner hair cells. Scale bars: 10 μ m.

mutant mice recovered to the same degree by 7 days after noise exposure for the high frequency stimuli, where the chosen noise exposure preferentially damaged the peripheral auditory system (i.e. thresholds were greater at the high versus the low frequency stimuli). Thus, upon challenging the auditory system with a loud noise exposure, both WT and $Cx43^{I130T/+}$ mutant mice have a similar susceptibility to noise-induced hearing loss.

DISCUSSION

It has been known for some time that Cx26 and Cx30 are essential for auditory function, as mutations in the genes encoding both of these connexins cause hearing loss. The role of Cx43 in hearing is far less clear although this connexin has been reported to be expressed at defined locations along both the peripheral and central auditory regions (Cohen-Salmon et al., 2004; Kim et al., 2013; Lautermann et al., 1998; Liu et al., 2014; Liu and Yang, 2015). Furthermore, two mutations in the gene encoding Cx43 (*GJA1*), L11F and V24A, have been identified in a cohort of patients with

non-syndromic hearing loss, providing a putative link between Cx43 and hearing loss (Liu et al., 2001). To ascertain whether Cx43 contributes to hearing, we used two genetically modified mouse lines that have been classically used to investigate the role of Cx43 in the developmental disorder known as oculodentodigital dysplasia (ODDD). We found that mice with the $Cx43^{I130T/+}$ mutation, which has been shown in other cell lines and tissue to retain ~50% of total Cx43 gap junction function (Kalcheva et al., 2007), have normal hearing that persisted in middle-aged mature mice (6 months of age). However, $Cx43^{G60S/+}$ mutant mice, which have been shown to have ~20% Cx43 function in other cell types and tissues (Flenniken et al., 2005), exhibit severe hearing loss and auditory brainstem (where Cx43 is expressed) neural firing deficits. Intriguingly, hearing loss was not attributed to loss of hair cell number or function, suggesting that the defect lies downstream of the organ of Corti (i.e. within the central neural pathway). When challenging the auditory system with exposure to a loud noise, $Cx43^{I130T/+}$ mutant mice exhibited a similar susceptibility to hearing impairment to

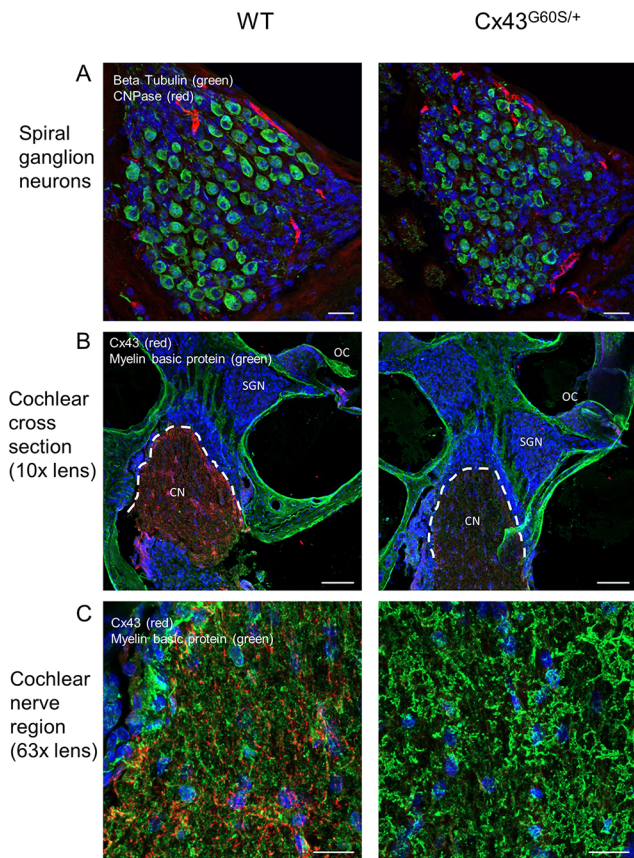


Fig. 7. Spiral ganglion neurons remain intact and there is no evidence of demyelination of the cochlear nerve in $Cx43^{G60S/+}$ mutant mice.

(A) Immunofluorescence confocal images of spiral ganglion neurons of WT and $Cx43^{G60S/+}$ mutant mice labelled for β -tubulin (neurons, green) and CNPase (Schwann cells, red). (B,C) Representative images of cochlear cross sections in WT and $Cx43^{G60S/+}$ mutant mice. Higher magnification images revealed abundant myelin, stained with myelin basic protein (green) in the cochlear nerve region (C). Note that Cx43 (red) is far less abundant in the cochlear nerve region of mutant mice compared to littermate controls (B,C). OC, organ of Corti; SGN, spiral ganglion neurons; CN, cochlear nerve. Scale bars: 20 μ m (A,C), 100 μ m (B).

their WT littermate controls, thereby meaning it is unlikely that Cx43 has a role in noise-induced hearing loss. Taken together, this study suggests that Cx43 is involved in the normal function of the auditory system.

Cx43 is the most ubiquitously expressed connexin family member and it has been linked to ODDD, a human disease that is inherited in mostly an autosomal-dominant manner (Paznekas et al., 2003). Patients with ODDD exhibit many different symptoms including craniofacial bone abnormalities, small eyes, enamel loss and fusion of soft tissue digits (Paznekas et al., 2003, 2009). In rare cases, patients can also exhibit neurological deficits and hearing loss, which has been found in ~7% of reported ODDD cases (Paznekas et al., 2009). Hearing loss in ODDD patients has been mostly attributed to conductive hearing loss, which is caused by abnormalities in either the outer or middle ear, where sound cannot adequately reach the cochlea, while others were reported to be due to central auditory deficits and a few remain idiopathic (Paznekas et al., 2009). However, it is currently unknown why some patients with ODDD exhibit hearing loss while others do not, and whether this is regulated by the functional status of Cx43. Thus, to examine Cx43 in the auditory system, we repurposed two different human

disease-linked mutant mouse models of ODDD, $Cx43^{I130T/+}$ and $Cx43^{G60S/+}$, that were previously used to study ODDD in a variety of tissues and organs (Flenniken et al., 2005; Kalcheva et al., 2007; Manias et al., 2008; Plante and Laird, 2008; Stewart et al., 2013). These two Cx43 mutants have distinct effects on Cx43 function. For example, when expressed alone in gap junction-deficient N2A or HeLa cells, the I130T mutant maintains residual gap junction channel function (Shibayama et al., 2005; Stewart et al., 2013) while the G60S mutant is functionally dead (Flenniken et al., 2005; McLachlan et al., 2008; Stewart et al., 2013). However, when the same mutants are expressed in cells that co-express WT or endogenous Cx43, the functional levels of total Cx43 channels are consistently reduced to ~50% (I130T) or ~20% (G60S) of the normal level reflecting their dominant behaviour on Cx43 (Flenniken et al., 2005; Kalcheva et al., 2007; Kozoriz et al., 2013; Manias et al., 2008; Plante and Laird, 2008; Stewart et al., 2013; Tong et al., 2009). Thus, although Cx43-based GJIC function has not been examined specifically in the auditory system (due to inaccessibility of the auditory tract for GJIC studies), we can extrapolate that the loss of Cx43 function in both mutant mice within Cx43-expressing cells of the auditory system should be similar to what has been previously reported. Therefore, using these two different mutant mice with both mild and severe loss of Cx43-based GJIC, we were able to assess how the level of functional Cx43 impacts hearing.

To our knowledge, only one study in mice has attempted to assess the role of Cx43 in hearing and they found that 3–4-month-old $Cx43^{+/-}$ mice had comparable hearing competence to controls, with a modest decrease in hearing capability in 10-month-old $Cx43^{+/-}$ mice (Kim et al., 2013). These findings are consistent with those in adult $Cx43^{I130T/+}$ mice, which did not have any significant hearing impairments, probably due to the fact that they also retained at least 50% normal Cx43 function. However, $Cx43^{G60S/+}$ mutant mice harbouring only ~20% Cx43-based GJIC had severe hearing loss, which was found to be ~60 dB across all sound frequencies. Hearing loss in $Cx43^{G60S/+}$ mutant mice was accompanied by decreases in all ABR waveform amplitudes, which indicates that there is a decreased neural synchrony and/or firing of downstream auditory brainstem regions because wave I represents the cochlear nerve activity and the subsequent waves (II–V) represent electrical activity in the subsequent relay nuclei of the central auditory pathway (Markand, 1994). In this manner, reductions of neural synchrony and/or firing could lead to inadequate transmission of auditory signals to the central auditory system. This finding suggests that Cx43 is involved in proper firing of neurons within the auditory brainstem nuclei, as mice with severe loss of Cx43 function exhibited significantly decreased ABR waveform amplitudes. A previous study reported a similar phenotype in $Cx29^{-/-}$ mice, where they had severe hearing loss and distorted ABR wave I amplitudes (Tang et al., 2006). Interestingly, Cx29 is expressed in the myelinating Schwann cells of the spiral ganglion neurons, whose axons are bundled together to form the cochlear nerve (i.e. represented by the ABR wave I). Upon further analysis, it was found that hearing loss and cochlear nerve defects in $Cx29^{-/-}$ mice was due to demyelinated auditory nerve fibres in the spiral ganglion neurons (Tang et al., 2006). Thus, the authors speculated that hearing loss in $Cx29^{-/-}$ mice was due to auditory neuropathy spectrum disorder, which is hearing loss in the presence of intact hair cells within the peripheral auditory system, but where there is abnormal transmission of sound conduction through the auditory nerve and to the brain within the central auditory system. Another gene linked to auditory neuropathy is Cx32; mutations in the gene

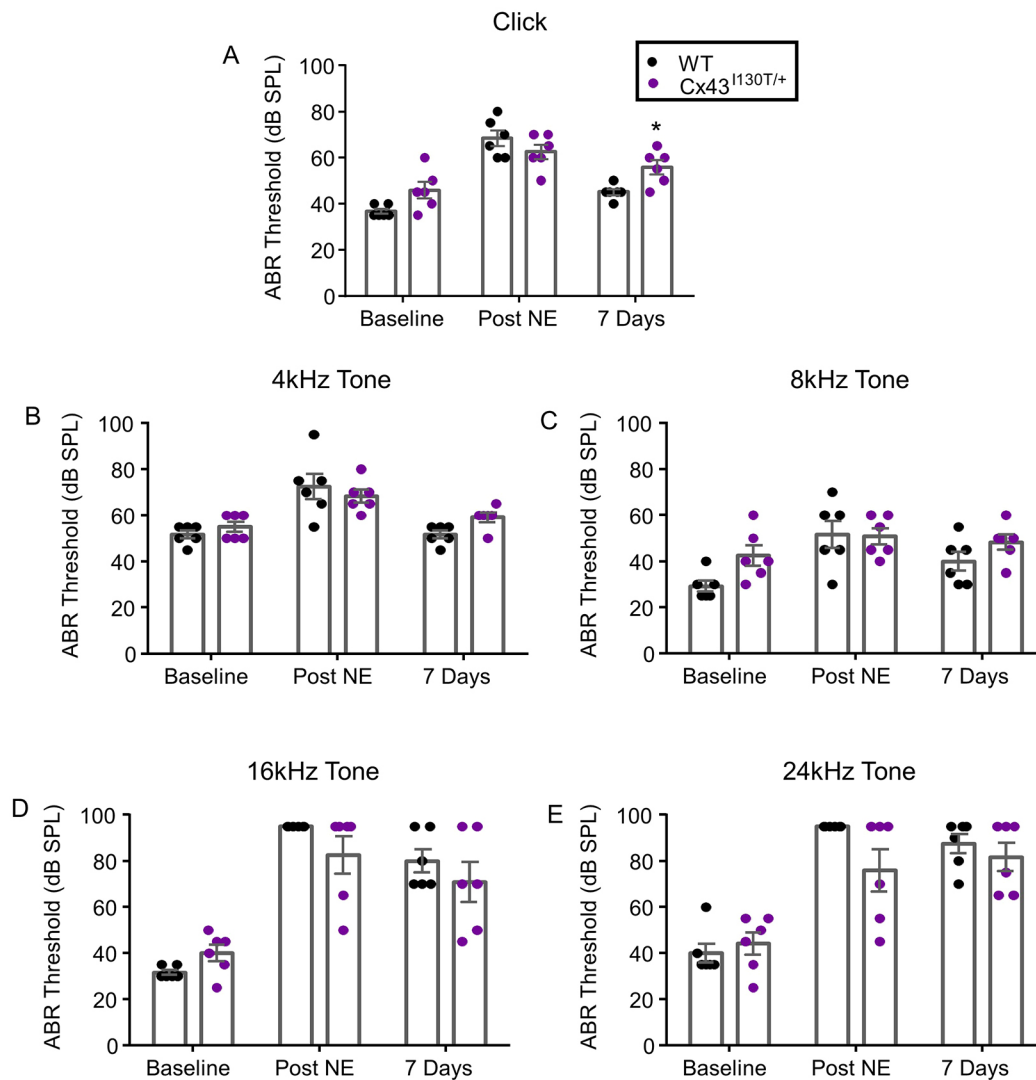


Fig. 8. Cx43^{I130T/+} mutant mice have a similar susceptibility to noise-induced hearing loss to that seen in control mice. (A–E) Noise exposure (NE) increased ABR thresholds immediately afterwards (Post NE) for all stimuli tested, confirming auditory damage in both WT and Cx43^{I130T/+} mutant mice. The highest ABR thresholds post NE were found at the higher frequency stimuli of (D) 16 kHz and (E) 24 kHz tones. There were no differences between the two groups at the higher frequency stimuli 7 days after NE (D,E). * $P < 0.05$ (two-way repeated-measures ANOVAs with a post hoc Sidak's test). $n = 6$ for both WT and Cx43^{I130T/+} mice. Bars represent the mean \pm s.e.m. ABR.

encoding Cx32 cause X-linked Charcot–Marie–Tooth disease (CMTX). In the auditory system, Cx32 is expressed in the stria vascularis (Degen et al., 2011) and in the cochlear nerve region near the glial juncture (Tang et al., 2006), where we have also found Cx43 to be expressed. Patients with CMTX also exhibit hearing loss in some cases, and this has been attributed to both cochlear and neural auditory pathologies (Papadakis et al., 2003; Rance et al., 2012). Thus, Cx29-, Cx32- and Cx43-induced hearing loss appear to manifest from abnormal transmission of sound to the higher-order centres of the auditory pathway, consistent with auditory neuropathy spectrum disorder.

To further elucidate the mechanism of hearing loss in Cx43^{G60S/+} mutant mice, we examined Cx43 expression and cell/tissue integrity using a top-to-bottom analysis of the auditory tract (from the peripheral auditory system, including the morphology of the cochlea, to the status of hair cells and spiral ganglion neurons, to the cochlear nerve region, and finally to the first part of the central auditory system). First, at the level of the cochlea, we found that

Cx43^{G60S/+} mutant mice did not exhibit hair cell loss, and these cells remained functional, as assessed via FM1-43 dye uptake through MET channels, which are essential for proper depolarization of hair cells. Upon examination of hair cells in 2–3-month-old adult mice, it was evident that the mechanism of hearing loss in Cx43^{G60S/+} mice was not due to mature hair cell loss. Likewise, further along the auditory tract, there was no evidence of spiral ganglion neuron degeneration in Cx43^{G60S/+} mutant mice compared to WT. Finally, we found that Cx43^{G60S/+} mutant mice had significantly decreased ABR wave amplitudes in all five waves, suggesting that neural synchrony is altered in the auditory brainstem regions where we and others (Kim et al., 2013) have shown Cx43 to be expressed. Decreases in the first ABR wave have been previously associated with auditory nerve fibre reductions, which can lead to hearing loss (Verhulst et al., 2016). However, Cx43^{G60S/+} mutant mice did not exhibit any differences in inner hair cell synapses, as was revealed by CtBP2 staining of ribbon synapses. Owing to the presence of an intact organ of Corti, the lack of hair cell loss and the high

abundance of Cx43 in the cochlear nerve, it is likely that the mechanism of hearing loss in Cx43^{G60S/+} mice is due to auditory brainstem neural deficits and is occurring downstream of the organ of Corti. Given the abundant expression of Cx43 gap junction plaques in the cochlear nerve region and the decreased ABR wave amplitudes, the most probable mechanistic site of hearing loss in Cx43^{G60S/+} mutant mice is in the cochlear nerve region.

In the auditory tract of young guinea pigs, rats and humans, Cx43 has been found in the satellite glial cells of the spiral ganglion neurons (Liu et al., 2009, 2014; Liu and Yang, 2015). In mice, a study showed that Cx43 was weakly expressed in the immature sensory epithelium until postnatal day 8 when Cx43 became exclusively localized to the cochlear bone (Cohen-Salmon et al., 2004). Recently, Cx43 has also been described in mice in the modiolus region of the cochlea as well as the higher auditory brainstem relays (Kim et al., 2013). The current study showed that Cx43 is found in gap junctions within the cochlear nerve region and surrounding astrocytic processes. This Cx43 localization pattern has also been shown in the brain where it is expressed among astrocytic processes that produce a glial syncytium network enabling a conduit for glial cell communication (Dermietzel et al., 1991; Giaume et al., 1997). The proposed role of Cx43 in these networks is to clear out waste materials such as excess neurotransmitter and K⁺ ions, and allow the passage of metabolites and ions from capillaries to neurons, as well as to recycle metabolites and ions that are important in normal neuronal homeostasis within the brain (Ball et al., 2007; Nagy and Rash, 2000; Saez et al., 2003). For example, one of the most prevalent roles of Cx43 in astrocytes of the brain is K⁺ buffering and clearance, where it is proposed to shuttle K⁺ ions from areas of high concentration to areas of low concentration to redistribute these excess ions arising from neural activity (Wallraff et al., 2006; Walz and Hertz, 1983). In this manner, Cx43 mediates homeostasis and alleviates toxicity as well as the build up of unwanted ions in the brain. Therefore, due to the prevalence of Cx43 around glial cells in the cochlear nerve regions and the decreased neural output of the auditory brainstem regions, we propose that Cx43 may be playing a similar role in the cochlear nerve region. More specifically, Cx43 gap junctions in this region could assist in maintaining ion homeostasis and dissipation of potentially harmful molecules such as overexposure to K⁺ ions or glutamate neurotransmitters, which have both been shown to cause hearing damage (Wong and Ryan, 2015). These Cx43-based gap junction channels would provide communication between glial cells of the cochlear nerve region and in turn could shuttle K⁺, glutamate, and other ions and neurotransmitters from areas of high to low concentrations to maintain proper cellular homeostasis within this auditory region, similar to the role of Cx43 in astrocytes of the brain. In turn, lack of efficient Cx43-based GJIC in astrocytes in the cochlear nerve could impede further conduction of auditory signals throughout subsequent brainstem relays.

Although studies have suggested a link between Cx43 and hearing, its involvement in noise-induced hearing loss is unknown. Both Cx26 and Cx30 are thought to play a role in the active transport of Na⁺ and K⁺ within the cochlea (Kikuchi et al., 2000a), and both Cx26 and Cx30 protein levels are significantly decreased after noise exposure (Yamaguchi et al., 2014). In addition, when Cx26 was conditionally knocked down at postnatal day 18, mice exhibited more pronounced noise-induced hearing loss than their WT counterparts (Zhou et al., 2016). In the present study, we sought to investigate the potential contributions of Cx43 to noise-induced hearing loss. When we challenged the auditory system of Cx43-compromised (~50% normal Cx43 function) Cx43^{I130T/+} mutant

mice with an acute loud noise, we found that there was no increase in susceptibility to noise trauma, or in recovery, when compared to littermate controls, unlike what has been shown for Cx26. The relative differences in the impact of noise exposure in mutant mice for these two different connexins may give us novel insights into their relative roles within the auditory tract. This suggests that Cx43 is not likely to be linked to noise-induced hearing loss as might be the case for Cx26.

In summary, it is well known that mutations in genes encoding connexin family members (such as Cx26 and Cx30) lead to mild, moderate and severe hearing loss (Cohen-Salmon et al., 2002; Crispino et al., 2011; Kudo et al., 2003; Sun et al., 2009; Teubner et al., 2003; Wang et al., 2009). Here, we have identified that Cx43^{G60S/+} mutant mice, which retain only ~20% normal Cx43 function, exhibit severe hearing loss and central auditory deficits, thereby expanding the list of connexin family members linked to hearing loss. We propose that Cx43 is essential in the propagation of sound from the cochlear nerve to the higher-order auditory regions and, thus, that a loss of Cx43-based GJIC results in abnormal transmission of sound conduction, similar to what is seen in auditory neuropathy spectrum disorders. Furthermore, we have found that a 50% reduction of Cx43 does not appear to play a role in noise-induced hearing loss in mice. Taken together, we have identified Cx43 function as being critically important in hearing, which may explain why some ODDD patients harbouring Cx43 mutants have the additional morbidity of hearing loss.

MATERIALS AND METHODS

Animals

Heterozygous mice harbouring the Cx43 I130T mutation (generously obtained from Glenn Fishman, New York University School of Medicine, New York, NY, USA) were created as previously described (Kalcheva et al., 2007) and were bred on a C57BL/6 background and backcrossed in house for over six generations. Both male Cx43^{I130T/+} mutant and WT littermate controls were used for our studies. Mutant mice were phenotyped by evident syndactyly of the digits, and all mice were genotyped. Heterozygote mice carrying the Cx43 G60S mutation (generously obtained from Janet Rossant, The Hospital for Sick Children, Toronto, ON, Canada) were created as previously described (Flenniken et al., 2005). These mice were on a mixed C3H/HeJ and C57BL/6 background, and Cx43^{G60S/+} mutant mice used in these studies were compared to their WT littermate controls. All mice tested were male and 2–3 months of age unless otherwise stated. Mice were housed in the animal care facilities at the University of Western Ontario, and maintained on a 12-h-light–12-h-dark cycle and fed *ad libitum*. All experiments were approved by the Animal Care Committee at the University of Western Ontario.

Ribonucleic acid extraction and RT-PCR

Following euthanasia by means of CO₂, cochleae were dissected from mice and flash-frozen in liquid nitrogen. Ribonucleic acid (RNA) was extracted from tissues using a combination of Trizol and a Qiagen RNeasy mini kit as was previously described (Abitbol et al., 2016). A NanoDrop spectrophotometer was used to measure the absorbance of RNA and a one-step RT-PCR was performed using an RT-PCR Qiagen kit. The PCR profile was as follows: 50°C for 30 min, 95°C for 15 min, 94°C for 30 s, 64°C for 30 s, and 72°C for 1 min for 30 cycles. Primers used were as follows: Cx43-specific primers, forward, 5'-ACAACAAGCAAGCCAGCGAG-3' and reverse, 5'-TCGTCAGGGAAATCAAACGG-3'; Cx26-specific primers, forward, 5'-CCGTCTTCATGTACGTCCTTTACAT-3' and reverse, 5'-ATACCTAACGAACAAATAGCACAGC-3'; and Cx30-specific primers, forward, 5'-GGCCGAGTTGTGTACCTGCT-3' and reverse, 5'-TCTCTTCAGGGCATGGTTGG-3'. 18S ribosomal ribonucleic acid (rRNA) was used as a housekeeping gene (forward, 5'-GTAACCCGTTGAACCCATT-3' and reverse, 5'-CCATCCAATCGGTA GTAGCG-3'). The amplified products were run on a 2% agarose gel with ethidium bromide for visualization.

qRT-PCR

Following euthanasia by means of CO₂, cochleae were dissected from mice and flash-frozen in liquid nitrogen. RNA was extracted and converted into cDNA as previously described (Abitbol et al., 2016). Two-step qRT-PCR were performed using a SYBR green PCR master mix (Life Technologies) in order to quantify Cx43, Cx26 and Cx30 expression. The PCR protocol for all primers were as follows: 50°C for 2 min, 95°C for 2 min, 95°C for 5 s, 60°C for 15 s, followed by a melt curve. The same primers as mentioned above were used for qRT-PCR and transcripts were normalized to 18S rRNA. Normalized mRNA expression levels were analysed using the $\Delta\Delta\text{CT}$ method, which was calculated using BioRad Software. A WT sample was set as the control for all calculations.

Immunoblotting

Following euthanasia by means of CO₂, a litter of mice (~6–10 cochleae) were dissected, flash frozen in liquid nitrogen and pooled together (due to small tissue sizes) for one lysate sample and stored at –80°C. Cochleae were crushed with a mortar and pestle with liquid nitrogen as previously described (Abitbol et al., 2016). Tissues were solubilized in RIPA buffer (50 mM Tris-HCl, 150 mM NaCl, 1% TritonX-100, 13 mM deoxycolate acid, 0.1% SDS) and 30 µg of lysate was subjected to SDS-PAGE (10% polyacrylamide gels) and transferred onto nitrocellulose membranes using an iBlot transfer apparatus (Invitrogen). Membranes were blocked with 3% bovine serum albumin (BSA) in PBS-Tween (1× phosphate-buffered saline with 0.05% Tween 20) for 1 h. Blots were probed overnight with rabbit anti-Cx43 (1:750, Sigma, catalog# C6219) and mouse anti-GAPDH (1:10,000 dilution, Chemicon, catalog# MAB374) antibodies. Blots were then washed and stained with Alexa Fluor 680-conjugated anti-rabbit-IgG secondary antibody (1:5000 dilution, Life Technologies) for Cx43 and IRdye800-conjugated anti-mouse-IgG antibody (1:5000, Rockland) for GAPDH for 2 h. Membranes were visualized with an Odyssey infrared imaging system (LiCor). Quantitative analysis was performed using Odyssey software to assess the amount of Cx43 total protein expression in 2–3-month-old mice. GAPDH was used as a loading control and a reference protein for quantitative analysis.

Immunofluorescence labelling

Following dissections of cochleae, a small incision was made in the cochlear bone near the apical turn and 4% paraformaldehyde (PFA) was perfused through both the round and oval windows of the cochlea. Cochleae were fixed in 4% PFA overnight at 4°C, then subsequently washed with PBS. Cochleae were then decalcified in 4% EDTA for 3 days and upon full decalcification were immersed in 30% sucrose overnight for cryopreservation of the tissue. Each pair of cochleae was embedded in an agarose solution, flash frozen, and allowed to acclimate in the cryostat at –25°C. Sections were cut at 18 µm thickness and stored at –20°C until use. Slides were blocked and permeabilized for 1 h in 3% BSA+ 0.02% Triton-X 100 solution. Subsequently, slides were incubated with primary antibodies in 4°C overnight. These antibodies included; rabbit anti-Cx43 (1:750, Sigma, catalog# C6219), mouse anti-CNPase (1:200, Millipore, catalog# MAB326), mouse anti-GFAP (1:200, Sigma, catalog# 63893), rabbit anti-myosin VI (1:200, Proteus Biosciences, catalog# 25-6791), mouse anti-CtBP2 (1:200, BD Transduction Laboratories, catalog#612044), mouse anti-myelin basic protein (1:200, Abcam, catalog# 62631), and rabbit anti-βIII tubulin (1:400, Abcam, catalog# 18207) antibodies. Slides were then washed and incubated with a fluorescent-conjugated secondary antibody, as well as phalloidin (1:400, Invitrogen, catalog #A12379) for 1 h following a nuclear Hoechst 33342 stain. Slides were then mounted and confocal immunofluorescence images were acquired using an LSM800 Zeiss confocal microscope.

Hearing assessment with the ABR

Hearing levels were determined using the ABR technique, which measures the electrical activity in the brainstem evoked by the repeated presentation of a given acoustic stimulus to ultimately assess hearing sensitivity. Five individual acoustic stimuli were used in our studies, which allowed us to test auditory function at various regions along the cochlea, which detect different sound frequencies. These stimuli included a broad-band click stimulus, which stimulates the 1–10 kHz frequency region of the cochlea, and four tonal-

specific stimuli of 4, 8, 16 and 24 kHz, in order to assess both broad-band as well as tonal-specific frequencies. In this manner, the low- to mid-frequency ranges spanning the apical and middle turns of the cochlea are tested. A detailed description of the experimental procedures for ABR recordings has been previously described (Abitbol et al., 2016). Briefly, mice were deeply anaesthetized with ketamine (100 mg/kg body weight) and xylazine (10 mg/kg body weight) administered via intraperitoneal injections, and electrical activity was recorded through subdermal electrodes placed at the vertex (active electrode), the mastoid of the stimulated ear (reference electrode) and on the mid-back (ground electrode). Mice were maintained at ~37°C on a digital homeothermic heating pad throughout the duration of the experiment. For ABR waveform analysis, BioSig software program was used to measure the amplitudes and latencies of 90 dB sound pressure level (SPL) click stimuli for each wave and each mouse group tested.

Noise exposures

For a separate cohort of mice at 1 month of age, an initial ABR experiment was followed immediately by a loud 12 kHz tonal stimulus at 115 dB SPL bilaterally for exposure in both ears for a 1 h time period as has been previously described (Abitbol et al., 2016). During the procedure, mice were deeply anaesthetized with ketamine (100 mg/kg body weight) and xylazine (10 mg/kg body weight), while noise exposures were performed in a sound attenuated chamber. Immediately following noise exposure, mice were reassessed with a second ABR to confirm elevation of thresholds at high frequencies following noise exposure. Mice were then administered antipamezole (1 mg/kg) to reverse the effects of anaesthesia and allowed to recover in their home cages. At 1 week after the noise exposure, a third and final ABR was performed to determine the extent of permanent hearing damage incurred after the loud noise exposure.

Organotypic cochlear cultures

Organotypic cochlear explant cultures were prepared from the cochleae of pups at P1–P3 and grown in MatTek dishes with glass coverslips as has been described (Russell and Richardson, 1987). Mouse pups were killed by cervical dislocation and were surface sterilized by immersion in 80% ethanol for 10 min. The heads were removed and placed in ice-cold Leibovitz L-15 medium (Invitrogen) where they were bisected midsagittally. The cochlear capsule was removed followed by the stria vascularis, leaving the organ of Corti and the epithelium. The explants were then plated in a MatTek dish containing a 14-mm diameter round glass coverslip that was coated with Cell Taq (Coming) for adhesion. Coverslips were immersed in 150 µl DMEM/F12 medium supplemented with 5% FBS (Invitrogen). Cultures were incubated at 37°C and 5% CO₂ for ~24 h. Cochlear cultures were fixed with 4% PFA, blocked for 1 h with 3% BSA plus 0.2% Triton-X 100 and subsequently incubated with an anti-myosin VI antibody (1:200, Proteus Biosciences) overnight at 4°C. Alexa Fluor-conjugated secondary antibody (1:1000, Invitrogen) was added to reveal labelling, in addition to an Alexa Fluor-conjugated phalloidin stain to visualize hair cell stereocilia. In addition, cultures were treated with the fluorescently labelled dye FM1-43, which is readily taken up by hair cells through the MET transduction channel. Cultures were loaded with FM1-43 dye for 30 s and were subsequently fixed with 4% PFA, then washed and mounted. Cultures were imaged using a Zeiss LSM800 high-resolution confocal microscopy. Images were acquired using a 25× objective lens, averaged four times, where 20 individual slices were taken and merged together for an averaged image.

Statistical analysis

Two-tailed independent unpaired Student's *t*-test were used for comparisons of connexin expression in the qRT-PCR as well as in Cx43 western blot (between WT and Cx43^{I130T/+} and WT and Cx43^{G60S/+} mice) experiments. Two-way analysis of variance (ANOVA) with Sidak's post hoc tests were used to compare different cohorts for the analyses of ABR threshold, the amplitudes and latencies of ABR waveform, hair cells counts and ABR thresholds for noise exposure analysis at each individual stimuli.

Acknowledgements

The authors would like to thank Dr Glenn Fishman and Dr Janet Rossant for providing the mutant mice.

Competing interests

The authors declare no competing or financial interests.

Author contributions

Conceptualization: J.M.A., J.J.K., B.L.A., D.W.L.; Methodology: J.M.A., D.W.L.; Validation: J.M.A., B.L.A.; Formal analysis: J.M.A., B.L.A., D.W.L.; Investigation: J.M.A., J.J.K., B.L.A.; Resources: K.J.B., D.W.L.; Data curation: J.J.K., K.J.B.; Writing - original draft: J.M.A.; Writing - review & editing: J.M.A., B.L.A., D.W.L.; Visualization: J.J.K.; Supervision: B.L.A., D.W.L.; Project administration: D.W.L.; Funding acquisition: B.L.A., D.W.L.

Funding

This work was supported by operating grants from the Canadian Institutes of Health Research to D.W.L. and B.L.A. (148584) and grant (137098) to B.L.A. J.M.A. was supported by a Natural Sciences and Engineering Research Council of Canada studentship.

Supplementary information

Supplementary information available online at <http://jcs.biologists.org/lookup/doi/10.1242/jcs.214635.supplemental>

References

- Abitbol, J. M., Kelly, J. J., Barr, K., Schormans, A. L., Laird, D. W. and Allman, B. L.** (2016). Differential effects of pannexins on noise-induced hearing loss. *Biochem. J.* **473**, 4665-4680.
- Anselmi, F., Hernandez, V. H., Crispino, G., Seydel, A., Ortolano, S., Roper, S. D., Kessar, N., Richardson, W., Rickheit, G., Filippov, M. A. et al.** (2008). ATP release through connexin hemichannels and gap junction transfer of second messengers propagate Ca²⁺ signals across the inner ear. *Proc. Natl. Acad. Sci. USA* **105**, 18770-18775.
- Ball, K. K., Gandhi, G. K., Thrash, J., Cruz, N. F. and Dienel, G. A.** (2007). Astrocytic connexin distributions and rapid, extensive dye transfer via gap junctions in the inferior colliculus: implications for [(14)C]glucose metabolite trafficking. *J. Neurosci. Res.* **85**, 3267-3283.
- Bosch, J., Lebeko, K., Nziale, J. J. N., Dandara, C., Makubalo, N. and Wonkam, A.** (2014). In search of genetic markers for nonsyndromic deafness in Africa: a study in Cameroonians and Black South Africans with the GJB6 and GJA1 candidate genes. *Omicron* **18**, 481-485.
- Bruzzo, R., White, T. W. and Paul, D. L.** (1996). Connections with connexins: the molecular basis of direct intercellular signaling. *Eur. J. Biochem.* **238**, 1-27.
- Chang, Q., Tang, W., Ahmad, S., Zhou, B. and Lin, X.** (2008). Gap junction mediated intercellular metabolite transfer in the cochlea is compromised in connexin30 null mice. *PLoS ONE* **3**, e4088.
- Cohen-Salmon, M., Ott, T., Michel, V., Hardelin, J.-P., Perfettini, I., Eybalin, M., Wu, T., Marcus, D. C., Wangemann, P., Willecke, K. et al.** (2002). Targeted ablation of connexin26 in the inner ear epithelial gap junction network causes hearing impairment and cell death. *Curr. Biol.* **12**, 1106-1111.
- Cohen-Salmon, M., Maxeiner, S., Kruger, O., Theis, M., Willecke, K. and Petit, C.** (2004). Expression of the connexin43- and connexin45-encoding genes in the developing and mature mouse inner ear. *Cell Tissue Res.* **316**, 15-22.
- Crispino, G., Di Pasquale, G., Scimemi, P., Rodriguez, L., Galindo Ramirez, F., De Siati, R. D., Santarelli, R. M., Arslan, E., Bortolozzi, M., Chiorini, J. A. et al.** (2011). BAAV mediated GJB2 gene transfer restores gap junction coupling in cochlear organotypic cultures from deaf Cx26Sox10Cre mice. *PLoS ONE* **6**, e23279.
- Degen, J., Schütz, M., Dicke, N., Strenzke, N., Jokwitz, M., Moser, T. and Willecke, K.** (2011). Connexin32 can restore hearing in connexin26 deficient mice. *Eur. J. Cell Biol.* **90**, 817-824.
- Dermietzel, R., Hertberg, E. L., Kessler, J. A. and Spray, D. C.** (1991). Gap junctions between cultured astrocytes: immunocytochemical, molecular, and electrophysiological analysis. *J. Neurosci.* **11**, 1421-1432.
- Flenniken, A. M., Osborne, L. R., Anderson, N., Ciliberti, N., Fleming, C., Gittens, J. E., Gong, X. Q., Kelsey, L. B., Lounsbury, C., Moreno, L. et al.** (2005). A Gja1 missense mutation in a mouse model of oculodentodigital dysplasia. *Development* **132**, 4375-4386.
- Forge, A., Becker, D., Casalotti, S., Edwards, J., Evans, W. H., Lench, N. and Souter, M.** (1999). Gap junctions and connexin expression in the inner ear. *Novartis Found. Symp.* **219**, 134-150; discussion 151-6.
- Giaume, C., Taberner, A. and Medina, J. M.** (1997). Metabolic trafficking through astrocytic gap junctions. *Glia* **21**, 114-123.
- Goodenough, D. A., Goliger, J. A. and Paul, D. L.** (1996). Connexons, connexons, and intercellular communication. *Annu. Rev. Biochem.* **65**, 475-502.
- Henry, K. R. and Chole, R. A.** (1980). Genotypic differences in behavioral, physiological and anatomical expressions of age-related hearing loss in the laboratory mouse. *Audiology* **19**, 369-383.
- Jagger, D. J. and Forge, A.** (2006). Compartmentalized and signal-selective gap junctional coupling in the hearing cochlea. *J. Neurosci.* **26**, 1260-1268.
- Jagger, D. J. and Forge, A.** (2015). Connexins and gap junctions in the inner ear—it's not just about K(+) recycling. *Cell Tissue Res.* **360**, 633-644.
- Johnson, S. L., Ceriani, F., Houston, O., Polishchuk, R., Polishchuk, E., Crispino, G., Zorzi, V., Mammano, F. and Marcotti, W.** (2017). Connexin-mediated signaling in nonsensory cells is crucial for the development of sensory inner hair cells in the mouse cochlea. *J. Neurosci.* **37**, 258-268.
- Kalcheva, N., Qu, J., Sandeep, N., Garcia, L., Zhang, J., Wang, Z., Lampe, P. D., Suadcani, S. O., Spray, D. C. and Fishman, G. I.** (2007). Gap junction remodeling and cardiac arrhythmogenesis in a murine model of oculodentodigital dysplasia. *Proc. Natl. Acad. Sci. USA* **104**, 20512-20516.
- Keithley, E. M., Canto, C., Zheng, Q. Y., Fischel-Ghodsian, N. and Johnson, K. R.** (2004). Age-related hearing loss and the ahl locus in mice. *Hear. Res.* **188**, 21-28.
- Kikuchi, T., Adams, J. C., Paul, D. L. and Kimura, R. S.** (1994). Gap junction systems in the rat vestibular labyrinth: immunohistochemical and ultrastructural analysis. *Acta Otolaryngol.* **114**, 520-528.
- Kikuchi, T., Kimura, R. S., Paul, D. L. and Adams, J. C.** (1995). Gap junctions in the rat cochlea: immunohistochemical and ultrastructural analysis. *Anat. Embryol.* **191**, 101-118.
- Kikuchi, T., Adams, J. C., Miyabe, Y., So, E. and Kobayashi, T.** (2000a). Potassium ion recycling pathway via gap junction systems in the mammalian cochlea and its interruption in hereditary nonsyndromic deafness. *Med. Electron. Microsc.* **33**, 51-56.
- Kikuchi, T., Kimura, R. S., Paul, D. L., Takasaka, T. and Adams, J. C.** (2000b). Gap junction systems in the mammalian cochlea. *Brain Res. Brain Res. Rev.* **32**, 163-166.
- Kim, A. H., Nahm, E., Sollas, A., Mattiace, L. and Rozental, R.** (2013). Connexin 43 and hearing: possible implications for retrocochlear auditory processing. *Laryngoscope* **123**, 3185-3193.
- Kozoriz, M. G., Lai, S., Vega, J. L., Sáez, J. C., Sin, W. C., Bechberger, J. F. and Naus, C. C.** (2013). Cerebral ischemic injury is enhanced in a model of oculodentodigital dysplasia. *Neuropharmacology* **75**, 549-556.
- Kudo, T., Kure, S., Ikeda, K., Xia, A. P., Katori, Y., Suzuki, M., Kojima, K., Ichinohe, A., Suzuki, Y., Aoki, Y. et al.** (2003). Transgenic expression of a dominant-negative connexin26 causes degeneration of the organ of Corti and non-syndromic deafness. *Hum. Mol. Genet.* **12**, 995-1004.
- Laird, D. W.** (1996). The life cycle of a connexin: gap junction formation, removal, and degradation. *J. Bioenerg. Biomembr.* **28**, 311-318.
- Laird, D. W.** (2006). Life cycle of connexins in health and disease. *Biochem. J.* **394**, 527-543.
- Lautermann, J., ten Cate, W.-J. F., Altenhoff, P., Grümmer, R., Traub, O., Frank, H.-G., Jahnke, K. and Winterhager, E.** (1998). Expression of the gap-junction connexins 26 and 30 in the rat cochlea. *Cell Tissue Res.* **294**, 415-420.
- Liu, W. J. and Yang, J.** (2015). Preferentially regulated expression of connexin 43 in the developing spiral ganglion neurons and afferent terminals in post-natal rat cochlea. *Eur. J. Histochem.* **59**, 2464.
- Liu, X. Z., Xia, X. J., Adams, J., Chen, Z. Y., Welch, K. O., Tekin, M., Ouyang, X. M., Kristiansen, A., Pandya, A., Balkany, T. et al.** (2001). Mutations in GJA1 (connexin 43) are associated with non-syndromic autosomal recessive deafness. *Hum. Mol. Genet.* **10**, 2945-2951.
- Liu, W., Boström, M., Kinnefors, A. and Rask-Andersen, H.** (2009). Unique expression of connexins in the human cochlea. *Hear. Res.* **250**, 55-62.
- Liu, W., Glueckert, R., Linthicum, F. H., Rieger, G., Blumer, M., Bitsche, M., Pechriggl, E., Rask-Andersen, H. and Schrott-Fischer, A.** (2014). Possible role of gap junction intercellular channels and connexin 43 in satellite glial cells (SGCs) for preservation of human spiral ganglion neurons: A comparative study with clinical implications. *Cell Tissue Res.* **355**, 267-278.
- Locher, H., de Groot, J. C. M. J., van Iperen, L., Huisman, M. A., Frijns, J. H. M. and Chua de Sousa Lopes, S. M.** (2015). Development of the stria vascularis and potassium regulation in the human fetal cochlea: Insights into hereditary sensorineural hearing loss. *Dev. Neurobiol.* **75**, 1219-1240.
- Manias, J. L., Plante, I., Gong, X.-Q., Shao, Q., Churko, J., Bai, D. and Laird, D. W.** (2008). Fate of connexin43 in cardiac tissue harbouring a disease-linked connexin43 mutant. *Cardiovasc. Res.* **80**, 385-395.
- Markand, O. N.** (1994). Brainstem auditory evoked potentials. *J. Clin. Neurophysiol.* **11**, 319-342.
- McLachlan, E., Plante, I., Shao, Q., Tong, D., Kidder, G. M., Bernier, S. M. and Laird, D. W.** (2008). ODDD-linked Cx43 mutants reduce endogenous Cx43 expression and function in osteoblasts and inhibit late stage differentiation. *J. Bone Miner. Res.* **23**, 928-938.
- Mikaelian, D. O.** (1979). Development and degeneration of hearing in the C57/b16 mouse: relation of electrophysiologic responses from the round window and cochlear nucleus to cochlear anatomy and behavioral responses. *Laryngoscope* **89**, 1-15.
- Nagy, J. I. and Rash, J. E.** (2000). Connexins and gap junctions of astrocytes and oligodendrocytes in the CNS. *Brain Res. Brain Res. Rev.* **32**, 29-44.
- Nickel, R. and Forge, A.** (2008). Gap junctions and connexins in the inner ear: their roles in homeostasis and deafness. *Curr. Opin Otolaryngol. Head Neck Surg.* **16**, 452-457.

- Papadakis, C. E., Haggiannou, J. K., Kyrnizakis, D. E. and Bizakis, J. G.** (2003). Bilateral sudden sensorineural hearing loss caused by Charcot-Marie-Tooth disease. *J. Laryngol. Otol.* **117**, 399-401.
- Paznekas, W. A., Boyadjiev, S. A., Shapiro, R. E., Daniels, O., Wollnik, B., Keegan, C. E., Innis, J. W., Dinulos, M. B., Christian, C., Hannibal, M. C. et al.** (2003). Connexin 43 (GJA1) mutations cause the pleiotropic phenotype of oculodentodigital dysplasia. *Am. J. Hum. Genet.* **72**, 408-418.
- Paznekas, W. A., Karczeski, B., Vermeer, S., Lowry, R. B., Delatycki, M., Laurence, F., Koivisto, P. A., Van Maldergem, L., Boyadjiev, S. A., Bodurtha, J. N. et al.** (2009). GJA1 mutations, variants, and connexin 43 dysfunction as it relates to the oculodentodigital dysplasia phenotype. *Hum. Mutat.* **30**, 724-733.
- Piazza, V., Ciubotaru, C. D., Gale, J. E. and Mammano, F.** (2007). Purinergic signalling and intercellular Ca²⁺ wave propagation in the organ of Corti. *Cell Calcium* **41**, 77-86.
- Plante, I. and Laird, D. W.** (2008). Decreased levels of connexin43 result in impaired development of the mammary gland in a mouse model of oculodentodigital dysplasia. *Dev. Biol.* **318**, 312-322.
- Rance, G., Ryan, M. M., Bayliss, K., Gill, K., O'Sullivan, C. and Whitechurch, M.** (2012). Auditory function in children with Charcot-Marie-Tooth disease. *Brain* **135**, 1412-1422.
- Reaume, A. G., de Sousa, P. A., Kulkarni, S., Langille, B. L., Zhu, D., Davies, T. C., Juneja, S. C., Kidder, G. M. and Rossant, J.** (1995). Cardiac malformation in neonatal mice lacking connexin43. *Science* **267**, 1831-1834.
- Russell, I. J. and Richardson, G. P.** (1987). The morphology and physiology of hair cells in organotypic cultures of the mouse cochlea. *Hear. Res.* **31**, 9-24.
- Saez, J. C., Contreras, J. E., Bukauskas, F. F., Retamal, M. A. and Bennett, M. V. L.** (2003). Gap junction hemichannels in astrocytes of the CNS. *Acta Physiol. Scand.* **179**, 9-22.
- Shibayama, J., Paznekas, W., Seki, A., Taffet, S., Jabs, E. W., Delmar, M. and Musa, H.** (2005). Functional characterization of connexin43 mutations found in patients with oculodentodigital dysplasia. *Circ. Res.* **96**, e83-e91.
- Stewart, M. K. G., Gong, X.-Q., Barr, K. J., Bai, D., Fishman, G. I. and Laird, D. W.** (2013). The severity of mammary gland developmental defects is linked to the overall functional status of Cx43 as revealed by genetically modified mice. *Biochem. J.* **449**, 401-413.
- Sun, Y., Tang, W., Chang, Q., Wang, Y., Kong, W. and Lin, X.** (2009). Connexin30 null and conditional connexin26 null mice display distinct pattern and time course of cellular degeneration in the cochlea. *J. Comp. Neurol.* **516**, 569-579.
- Tang, W., Zhang, Y., Chang, Q., Ahmad, S., Dahlke, I., Yi, H., Chen, P., Paul, D. L. and Lin, X.** (2006). Connexin29 is highly expressed in cochlear Schwann cells, and it is required for the normal development and function of the auditory nerve of mice. *J. Neurosci.* **26**, 1991-1999.
- Teubner, B., Michel, V., Pesch, J., Lautermann, J., Cohen-Salmon, M., Sohl, G., Jahnke, K., Winterhager, E., Herberhold, C., Hardelin, J. P. et al.** (2003). Connexin30 (Gjb6)-deficiency causes severe hearing impairment and lack of endocochlear potential. *Hum. Mol. Genet.* **12**, 13-21.
- Tong, D., Lu, X., Wang, H.-X., Plante, I., Lui, E., Laird, D. W., Bai, D. and Kidder, G. M.** (2009). A dominant loss-of-function GJA1 (Cx43) mutant impairs parturition in the mouse. *Biol. Reprod.* **80**, 1099-1106.
- Uyguner, O., Emiroglu, M., Uzumcu, A., Hafiz, G., Ghanbari, A., Baserer, N., Yuksel-Apak, M. and Wollnik, B.** (2003). Frequencies of gap- and tight-junction mutations in Turkish families with autosomal-recessive non-syndromic hearing loss. *Clin. Genet.* **64**, 65-69.
- Verhulst, S., Jagadeesh, A., Mauermann, M. and Ernst, F.** (2016). Individual differences in auditory brainstem response wave characteristics: relations to different aspects of peripheral hearing loss. *Trends Hear.* **20**, 2331216516672186.
- Verselis, V. K.** (2017). Connexin hemichannels and cochlear function. *Neurosci. Lett.* **S0304-3940(17)30754-1**.
- Wallraff, A., Kohling, R., Heinemann, U., Theis, M., Willecke, K. and Steinhauser, C.** (2006). The impact of astrocytic gap junctional coupling on potassium buffering in the hippocampus. *J. Neurosci.* **26**, 5438-5447.
- Walz, W. and Hertz, L.** (1983). Functional interactions between neurons and astrocytes. II. Potassium homeostasis at the cellular level. *Prog. Neurobiol.* **20**, 133-183.
- Wang, Y., Chang, Q., Tang, W., Sun, Y., Zhou, B., Li, H. and Lin, X.** (2009). Targeted connexin26 ablation arrests postnatal development of the organ of Corti. *Biochem. Biophys. Res. Commun.* **385**, 33-37.
- Wong, A. C. and Ryan, A. F.** (2015). Mechanisms of sensorineural cell damage, death and survival in the cochlea. *Front. Aging Neurosci.* **7**, 58.
- Wonkam, A., Bosch, J., Noubiap, J. J. N., Lebeko, K., Makubalo, N. and Dandara, C.** (2015). No evidence for clinical utility in investigating the connexin genes GJB2, GJB6 and GJA1 in non-syndromic hearing loss in black Africans. *S. Afr. Med. J.* **105**, 23-26.
- Yamaguchi, T., Nagashima, R., Yoneyama, M., Shiba, T. and Ogita, K.** (2014). Disruption of ion-trafficking system in the cochlear spiral ligament prior to permanent hearing loss induced by exposure to intense noise: possible involvement of 4-hydroxy-2-nonenal as a mediator of oxidative stress. *PLoS ONE* **9**, e102133.
- Yang, J.-J., Huang, S.-H., Chou, K.-H., Liao, P.-J., Su, C.-C. and Li, S.-Y.** (2007). Identification of mutations in members of the connexin gene family as a cause of nonsyndromic deafness in Taiwan. *Audiol. Neurootol.* **12**, 198-208.
- Zhao, H.-B. and Santos-Sacchi, J.** (1999). Auditory collusion and a coupled couple of outer hair cells. *Nature* **399**, 359-362.
- Zhou, X.-X., Chen, S., Xie, L., Ji, Y.-Z., Wu, X., Wang, W.-W., Yang, Q., Yu, J.-T., Sun, Y., Lin, X. et al.** (2016). Reduced connexin26 in the mature cochlea increases susceptibility to noise-induced hearing loss in mice. *Int. J. Mol. Sci.* **17**, 301.